Tellus (1992), *44A*, 81–99

A most beautiful polar low. A case study of a polar low development in the Bear Island region

By THOR ERIK NORDENG, *The Norwegian Meteorological Institute, P.O. Box 43-Blindern, N-0313 Oslo, Norway*, and ERIK A. RASMUSSEN, *Geophysical Institute, Meteorological Division, University of Copenhagen, Haraldsgate 6, DK-2200 Copenhagen N, Denmark*

(Manuscript received 29 October 1990; in final form 14 October 1991)

ABSTRACT

Satellite images from 26 and 27 February 1987 of the Bear Island region show the formation of a polar low with an unusual symmetric cloud field around a central eye, which strongly resembles a small-scale tropical storm. Conventional observations as well as output from a limited area numerical model are scrutinized to understand the dynamics of the low and to determine whether the development and structure of the polar low actually corresponds to that of a tropical cyclone. The discussion is based upon potential vorticity arguments. The data shows that the analogy between this particular polar low and tropical storms is not limited to the structure of the cloud field. However, the low develops in a baroclinic environment and is triggered by an upper-level potential vorticity anomaly. The upper level forcing diminishes after the initial triggering phase. The possibility of a self-induced development during the maintenance phase from the release of latent heat is discussed.

1. Introduction

The idea that some polar lows are similar in their structure and dynamics to tropical cyclones goes back to Økland (1977) and Rasmussen (1977, 1979). Several important features such as deep convection, "warm cores", as well as "eyes" are common to both systems. For a detailed discussion of the similarities between polar lows and tropical systems the reader is referred to Emanuel and Rotunno (1989) and Rasmussen (1989). Emanuel and Rotunno proposed, based on theoretical considerations and modelling studies, "that at least some polar lows are indeed arctic hurricanes", and Rasmussen in his work took the same position based mainly on observations. Based on studies of cyclone developments in a semigeostrophic model, Montgomery and Farrel (1991) suggested that (some) polar low developments consist of an initial baroclinic growth phase followed by a prolonged slow intensification due to diabatic effects.

On the other hand it is a fact that most polar lows when viewed from a satellite do *not* resemble small hurricanes in any striking way. Some do, however, as for example the polar low to be discussed in this paper. From early on in its life the low already showed a high degree of axial symmetry around a central "eye", and later on a characteristic spiral structure like that observed in tropical cyclones developed as well. To the authors knowledge no other satellite image of a polar low so far observed has shown such a striking similarity to a small hurricane. Provoked by the striking similarity it was decided to investigate whether this system indeed should be considered to be equivalent to a tropical storm. The following discussion summarizes the results of this investigation.

In Section 2, we will describe the initial development and mature phase of the low as inferred from synoptic data and satellite images. In Section 3, we will consider the detailed surface wind and pressure field associated with the mature polar low, as well as the "landfall-phase". In Section 4, the development will be discussed by means of

Tellus A/44/2-1

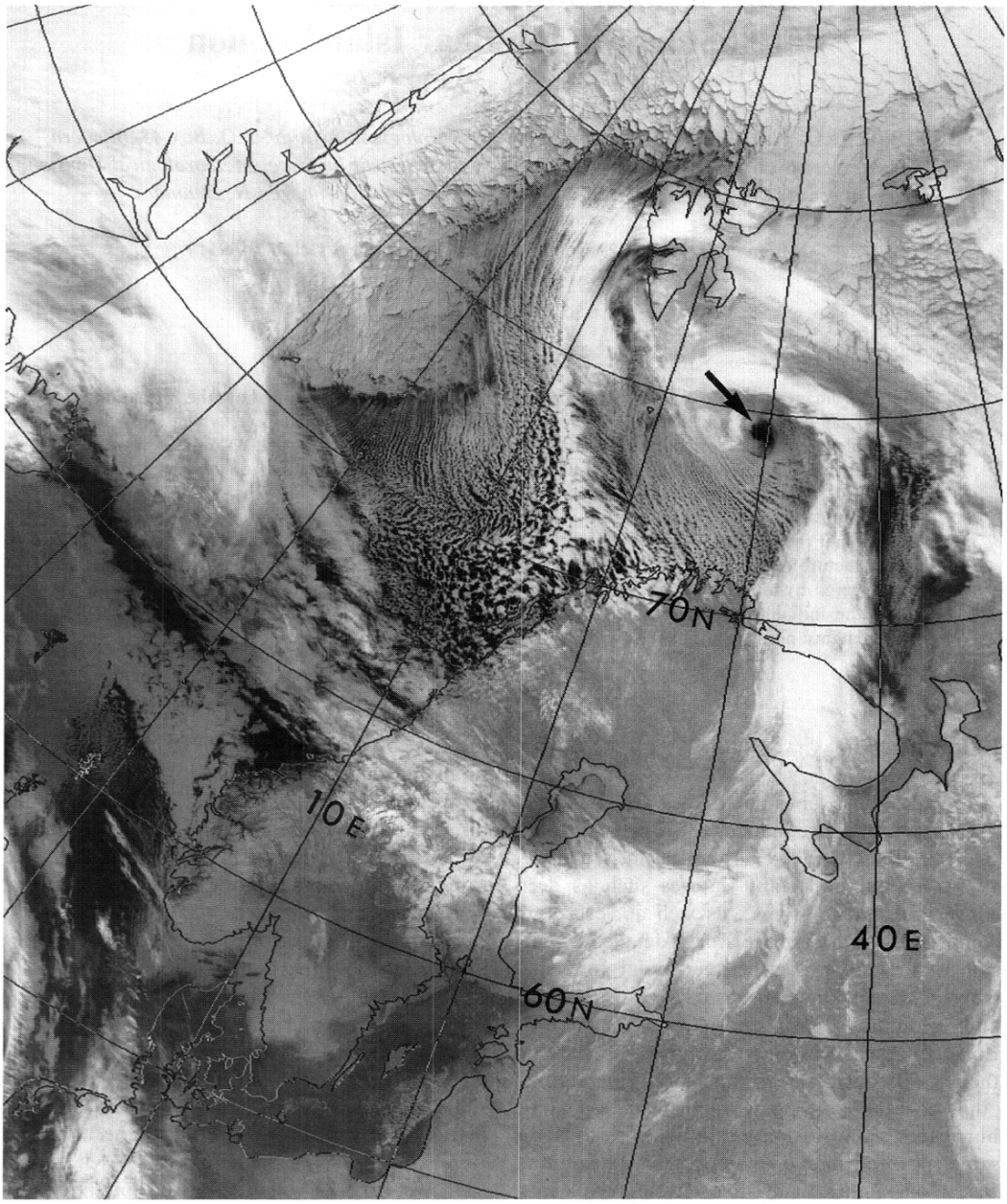

Fig. 1. NOAA-9 satellite image (infrared, Channel 4) 1244 UTC 26 February 1987 showing the incipient stage of the polar low which forms around the central dark eye (marked by arrow). Photograph courtesy of Department of Electrical Engineering and Electronics, University of Dundee.

model diagnostics from the Norwegian LAM (Limited Area Model). Finally, in Section 5, a discussion and some conclusions are presented.

2. A synoptic/satellite image-based study of the development

Satellite images and synoptic maps show that the precursor of the polar low development on 26 and 27 February 1987 was a small-scale cyclone situated over the Norwegian Sea on 25 February 1987. Satellite images (not reproduced) showed an open wave cyclone centred around 67°N, 0°E around noon 25 February as well as an extended upper level cloud deck further north. During the next 12 to 24 hours the cyclone occluded, resulting in the formation of a synoptic scale low with a central pressure around 995 hPa situated over the Barents Sea near 74°N, 30°E. Fig. 1 shows a satellite image of the occluded low at 1244 UTC on 26 February 1987.

On a satellite image about 4 h later at 1702 UTC (Fig. 2), most of the high clouds around the centre had disappeared. The low level clouds indicate the continued presence of a low level vortex with convective bands spiralling towards the centre. A ship about 200 km west of the centre observed a northerly wind at this time of around 30 m/s.

The position of the centre of the vortex at 74°N, 28°E corresponds closely to that computed from the model after 6 h of integration (Fig. 9a to follow). Radiosonde ascents from nearby Bear Island show that the surface layer in the region where the vortex formed is capped by a pronounced inversion which inhibited deep convection to

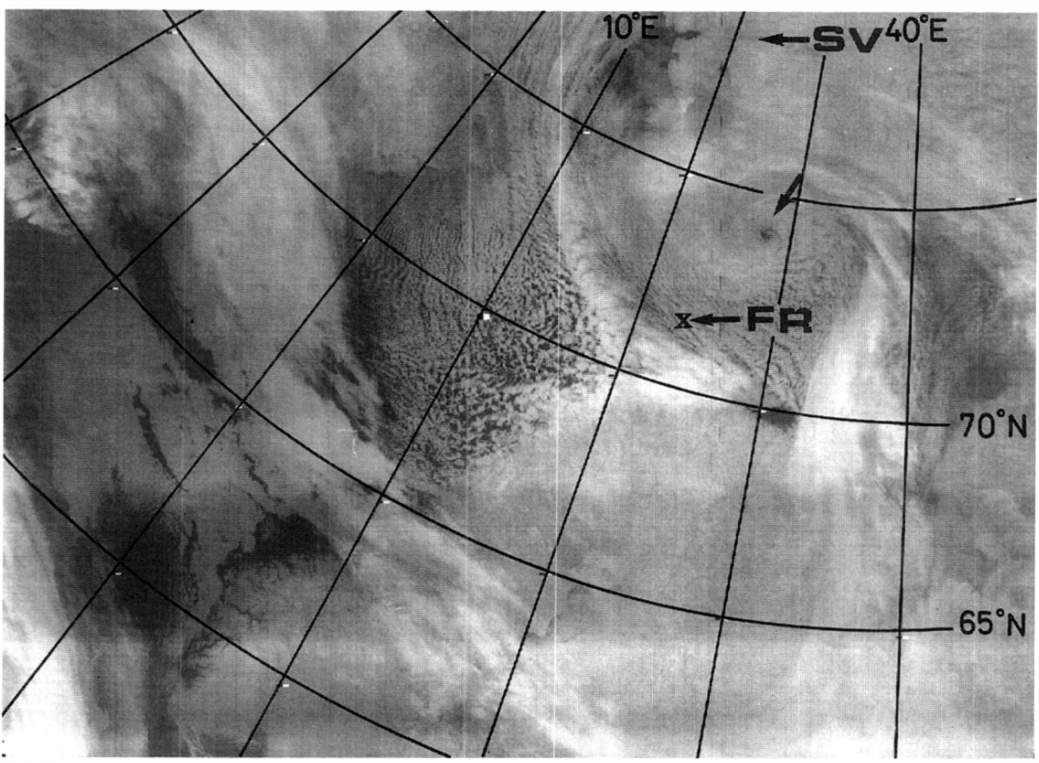

Fig. 2. NOAA-10 satellite image (infrared, Channel 4) 1702 UTC 26 February 1987 showing a cloud spiral (marked by arrow) of low level clouds associated with the polar low. Svalbard in the upper part of the picture has been marked by SV, and Fruholmen Lighthouse with FR. Photograph courtesy of Observatory of Space Research, The Danish Meteorological Institute, Rude Skov, Copenhagen.

develop (not shown). Due to the confinement of the clouds to the lowest 100 hPa or so the vortex looked different from most other incipient polar lows in that bands or clusters of deep convection were not present at this early stage of development. In the region, west and southwest of the centre, over the sea, strong cold air advection was occurring. The air in the region east of the cyclone, characterized by shallow convection, had been modified by the strong surface fluxes. Whether the shallow baroclinic field between the fresh cold air to the north and west of the low, and the modified warmer air mainly to the east helped trigger the development of the system will be discussed in Section 4.

Theoretical investigations have shown that the environment of polar lows normally is stable to small amplitude perturbations, and that, in order for polar lows to grow, disturbances of substantial amplitude appear to be necessary to initiate intensification through either CISK or air-sea interaction (Van Delden, 1989ab; Emanuel and Rotunno, 1989).

No satellite images are available between 1702 UTC on 26 February and the following morning 0244 UTC on 27 February. During these hours the centre of the low moved around 300 km from 74°N, 29°E to 73°N, 25°E and the low evolved into an intense small scale cyclone as seen from satellite pictures. The clouds were no longer

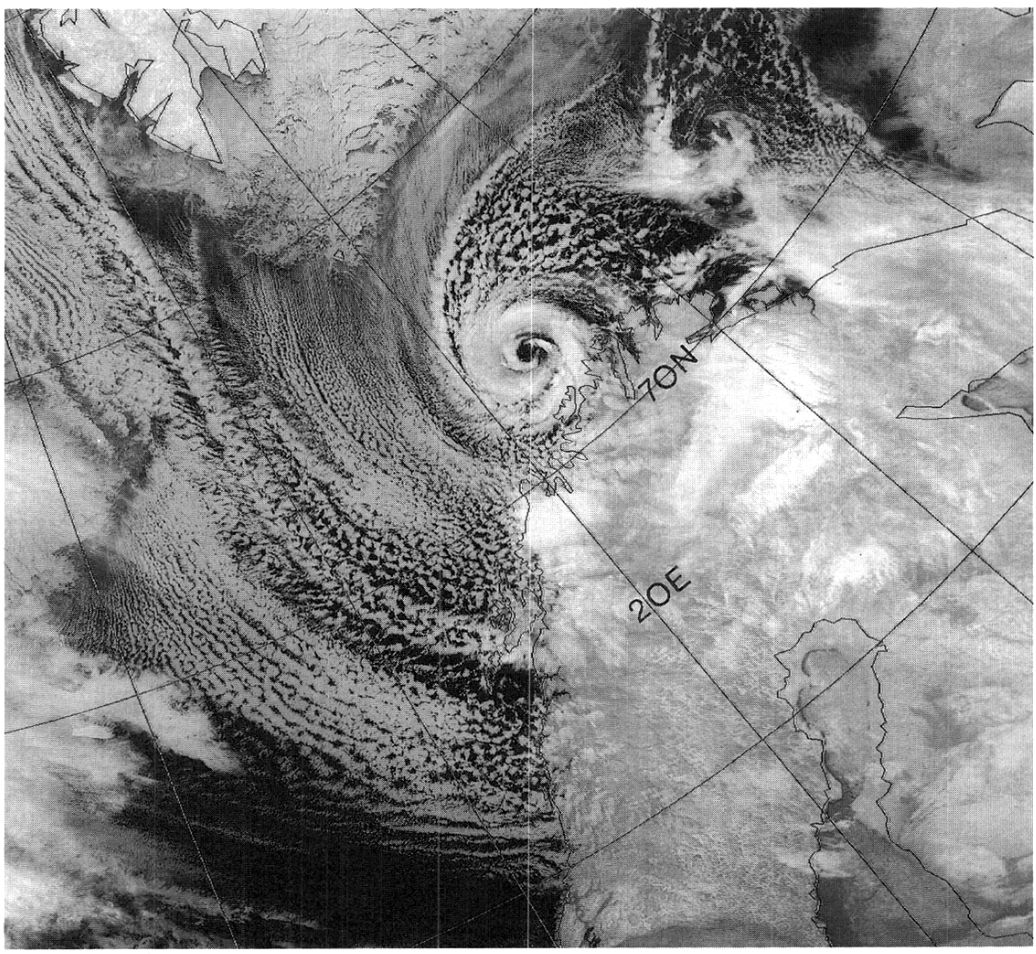

Fig. 3. NOAA-9 satellite image (infrared, Channel 4) 0831 UTC 27 February 1987 showing the polar low just before landfall. Photograph courtesy of Department of Electrical Engineering and Electronics, University of Dundee.

confined to a shallow layer near the surface and well developed spiral arms had formed. The satellite image shown on Fig. 3 from 0418 UTC 27 February 1987 is in all respects (except from a slight difference in the centre position) similar to the one from 0244 UTC. The satellite image shows:

- a striking similarity to tropical cyclones;
- regions of deep convection in the spiral arms;
- a well-defined eye of a rather large diameter;
- air mass contrasts across the spiral arms.

One important difference, however, between this polar low and its tropical counterparts was the contrasting air masses in the boundary layer. These contrasting air masses are very obvious from the structure of the cloud fields. From the satellite imagery one notes that the northern spiral arm separated a shallow and very cold air mass from a region of warmer air with cellular convection. The formation of the arms can be ascribed to the effect of confluence in the low level baroclinic zone found along the ice-edge (for a detailed discussion see Section 4). Generally low level fronts, i.e., arctic fronts, are known to develop when shallow arctic air masses are advected from the snow and ice covered regions out over the relatively warm sea surface as for example in this case on the western flank of the polar low.

3. The landfall

Immediately after landfall, the polar low lost it hurricane-like structure and well-defined eye as illustrated by Fig. 4 from 0831 UTC 27 February, i.e., only few hours after the centre crossed the coastline.

The low crossed the coast around 0600 UTC 27 February 1987 after the centre had passed Fruholmen lighthouse (71.1 N, 24.0 E north off the main coast) a short time before. The network of synoptic stations along the coast and inland is good, and even though the well defined spiral structure of the polar low disappeared very quickly after landfall (Fig. 5), the data from the coastal stations nevertheless show the surface pressure perturbation as well as the wind field of the mature polar low. The minimum pressure in the centre was very modest, only a little below 1000 hPa, and there was no indication of a strong (surface) pressure gradient close to the centre. Correspondingly the strongest surface winds at this time, around 20 m/s, are not observed close to the centre as we might expect but 200 km away on the western flank of the low.

The barogram traces from Fruholmen lighthouse as well as from some other stations close to the position where the landfall took place have been shown schematically on Fig. 6. The figure shows that the pressure disturbance associated with the polar low was of the order 5 hPa and that the low had a horizontal scale of a few hundred km at landfall. In addition to the barograph traces, available information on the maximum wind velocity for each of the stations is indicated on the figure. The highest wind velocity measured during the polar low passage was 19 ms^{-1} measured (as might be expected) at Fruholmen.

The low decays rapidly after landfall. This is evident from the comparison between Fig. 3 and Fig. 4. The surface map three hours after landfall at 0900 UTC (not shown) illustrates the changes induced by the landfall as well. Although the cyclonic circulation at this time is still clearly discernible, the low had already filled about 5 hPa. Even in this phase of rapid decay the disturbance could be followed most of the day as it crossed northern Sweden and the Gulf of Bothnia. One of the most remarkable features of the low at this stage were the marked pressure rise behind it which caused the wind locally to increase to around 20 ms^{-1}.

4. Numerical diagnostics

To study the development of this low in detail, we have used the mesoscale numerical model of The Norwegian Meteorological Institute (DNMI). The model is briefly described in Table 1. It is basically the operational weather prediction model at DNMI, except for minor changes made for this special simulation; the horizontal resolution is 25 km and the number of levels is 18 in the vertical. The sea surface temperature and ice border (Fig. 7) are based upon a subjective analysis. The initial analysis (Fig. 8) is the operational (50 km resolution) objective analysis at DNMI (Bratseth, 1986; Grønås and Midtbø, 1987). At the lateral

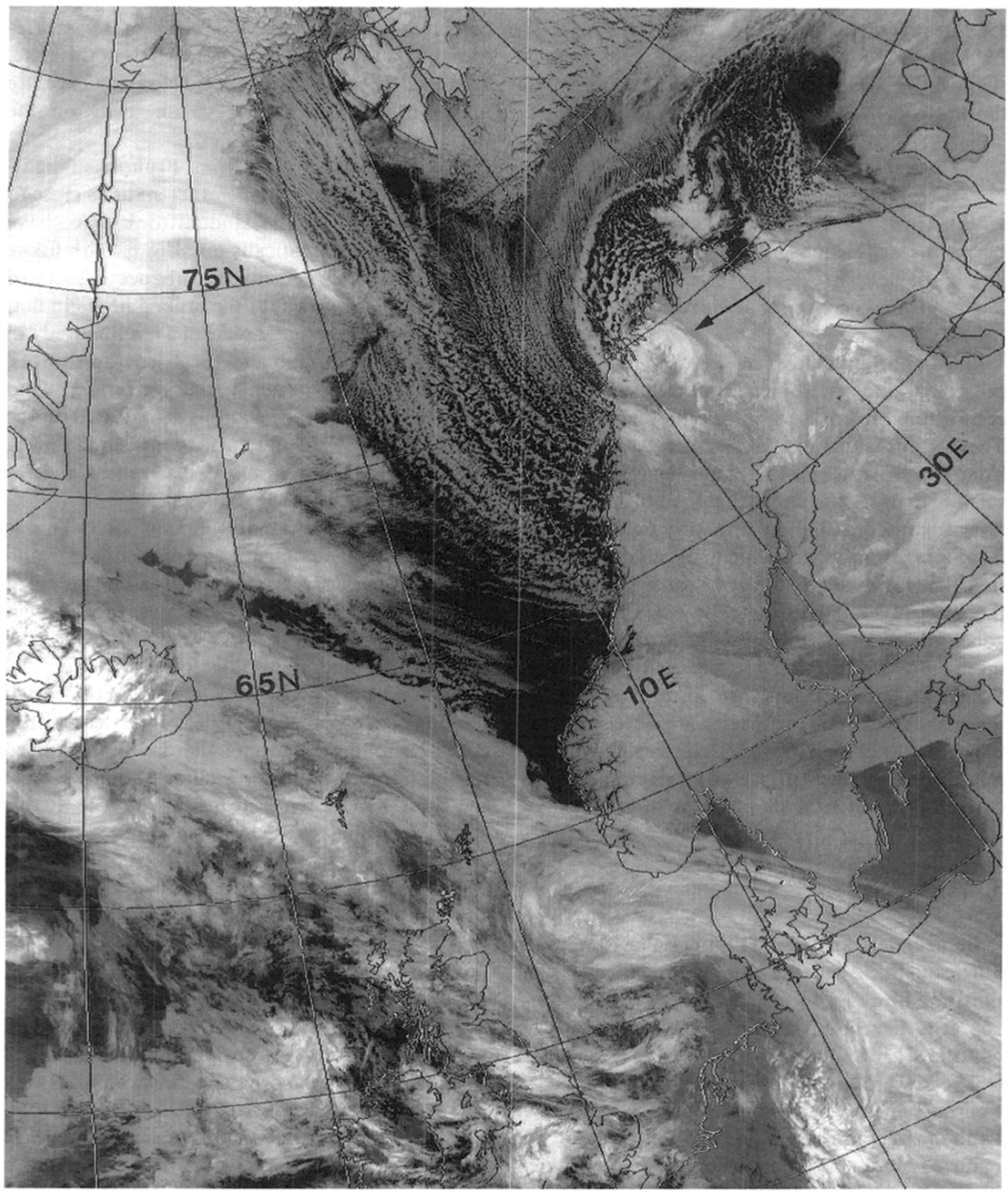

Fig. 4. NOAA-10 satellite image (infrared, Channel 4) 0831 UTC 27 February 1987 showing the polar low (marked by arrow) immediately after landfall. Photograph courtesy of Department of Electrical Engineering and Electronics, University of Dundee.

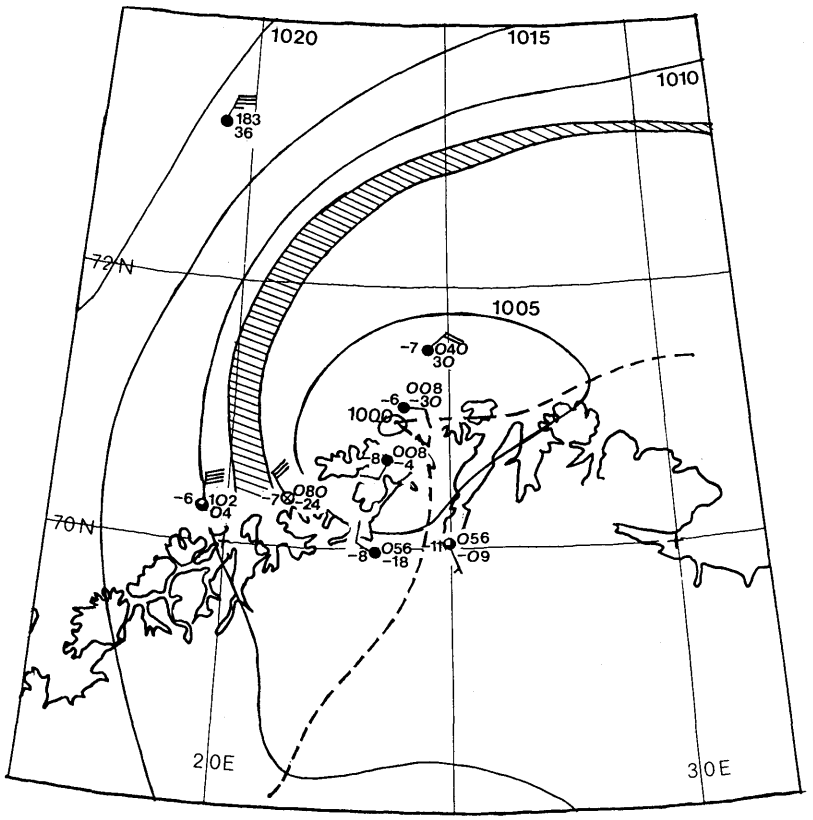

Fig. 5. Surface map 0600 UTC 27 February 1987. The position of the spiral cloud band taken from satellite image from 0551 UTC and seen on Figs. 3 and 4 has been indicated by hatching.

Table 1. *The mesoscale model (Grønås and Hellevik, 1982; Nordeng, 1986; Nordeng et al., 1988)*

*	Explicit time integration (Bratseth, 1983)
*	Dynamic initialization (Bratseth, 1982)
*	σ-coordinates, 18 levels $\Delta x = 25$ km, Arakawa D-grid
*	Surface fluxes (Louis et al., 1981) Exchange coefficient scheme, $K = K(\mathrm{Ri})$, for planetary boundary layer fluxes (Blackadar, 1979)
*	Land surface temperature and moisture equations (Nordeng, 1986).
*	Radiation/clouds (Nordeng, 1986)
*	Stratiform condensation/cloud liquid water (Nordeng, 1986)
*	Convection (Geleyn, 1985)
*	No explicit horizontal diffusion, implicit diffusion inherent in time-integration scheme affecting mainly $L < 3\,\Delta x$ waves.

boundaries updated 50 km resolution analyses are used as well throughout the integration. This model in the operational version was used by Nordeng (1990) to study the role of baroclinic energy release versus diabatic heating for the dynamics of two polar lows in the Norwegian Sea. Keyser and Uccellini (1987) have reviewed the application of mesoscale models for obtaining high resolution data (in space and time) for diagnostic studies.

It should be stressed that the Bratseth (1983) time integration scheme gives an effective horizontal resolution (as compared with the C-scheme) of $2^{-1/2}\,\Delta x$ for *all* derivatives of the governing equations. The diagnostics are performed with the AFOSS (developed by Mr. Anstein Foss at DNMI) a fully interactive colour plot system for model variables and derived variables in p or

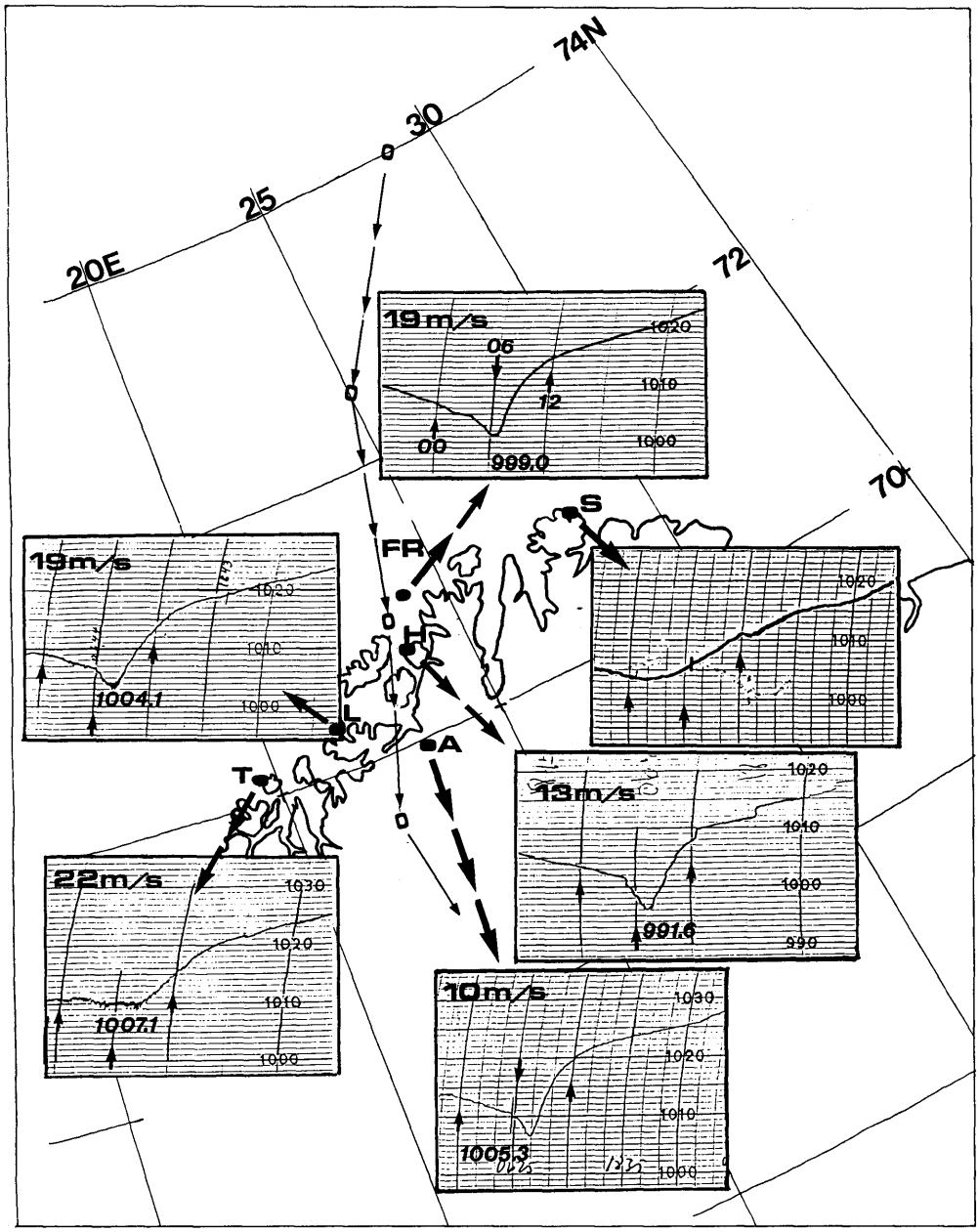

Fig. 6. Barogram curves and maximum mean winds (upper left corner) during passage of polar low for selected coastal stations in northern Norway. The pressure $p_0p_0p_0$ (in hPa) given for each station is the pressure at station level at 0600 UTC 27 February 1987. The track of the low is shown by the thin arrows. The short black arrows on the barograms indicate 000, 0600, and 1200 UTC 27 February 1987.

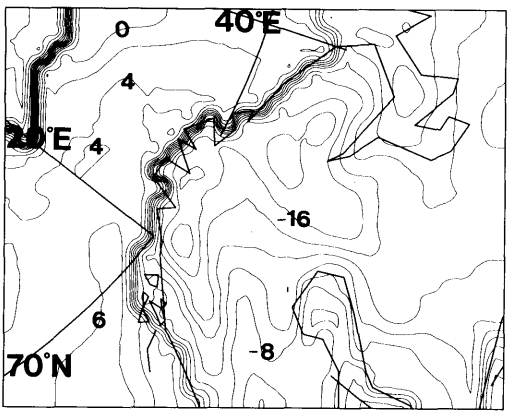

Fig. 7. The integration area. Surface temperatures at contour intervals of 2 °C at the beginning of the simulation. The sea surface temperatures are kept constant during the integration.

σ-surfaces, vertical sections, meteograms and soundings.

Fig. 9 shows the evolution of the low as described with the model over a 18 hr period from 1800 UTC 26 February 1987 to 0600 UTC 27 February 1987. We notice that a mesoscale low develops in the north-western part of the parent low, and moves anti-clockwise while it deepens. After 18 h of integration, the low makes landfall after which it quickly disappears. The central pressure during landfall (03 UTC 27 February) is 997 hPa, which should be compared with the observations of 994 hPa from Fruholmen lighthouse (71.1 N, 24.0 E). The model description of the low as compared with this observation, clouds from satellite pictures versus model precipitation, and model versus observed winds confirm that we can use the model diagnostics to try to understand the physics leading to the development of the low. It should be stressed however, that there is some noise in the simulation. This can be seen in Fig. 9c where the model actually predicts the development of three polar lows. The easternmost (along the coast) can be verified from satellite pictures, while the northern low is artificial. A closer inspection of this low reveals that it is due to interaction between convection and surface moisture flux at a scale that is not properly resolved by the model. It is however, quickly diffused by the implicit horizontal diffusion of the time integration scheme, and we have confidence that the evolution of the main low is not affected in any serious way. Lorenzo Dell'Osso (personal communication) at The European Centre for Medium Range Weather Forecasts (ECMWF) has run this case by using ECMWF's spectral limited area model with effective resolution of approximately 10 km, and his results confirm the results obtained here.

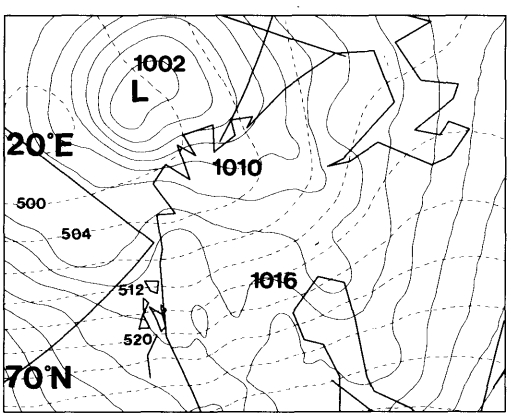

Fig. 8. Mean sea level pressure at contour intervals of 2 hPa (full lines) and geopotential height of 500 hPa at contour intervals of 40 m at the start of the integration (1200 UTC 26 February 1987).

The following analysis will show that a number of physical mechanisms are important for the development of this low. The low looks very symmetric in the satellite pictures with a striking resemblance to a tropical hurricane (except for the much larger "eye" as compared to the overall scale of the low). However, the analysis shows that the asymmetry of the "parent" low may be important for the development of the mesoscale low.

4.1. The rôle of potential vorticity anomalies

Fig. 9a shows mean sea level pressure close to the surface after 6 h of integration for a section of the whole integration area. There is cold air advection in the strong flow at the northwestern flank of the parent low, but very weak winds at the centre of the low. This leads to frontogenesis. The flow is quite strong (wind speeds up to 30 m/s), and the fluxes of heat and moisture from the ocean are large as well, partly due to the strong wind, but also from the large temperature difference between the warm ocean and the cold air. Fig. 10 shows the surface fluxes of latent and sensible heat combined.

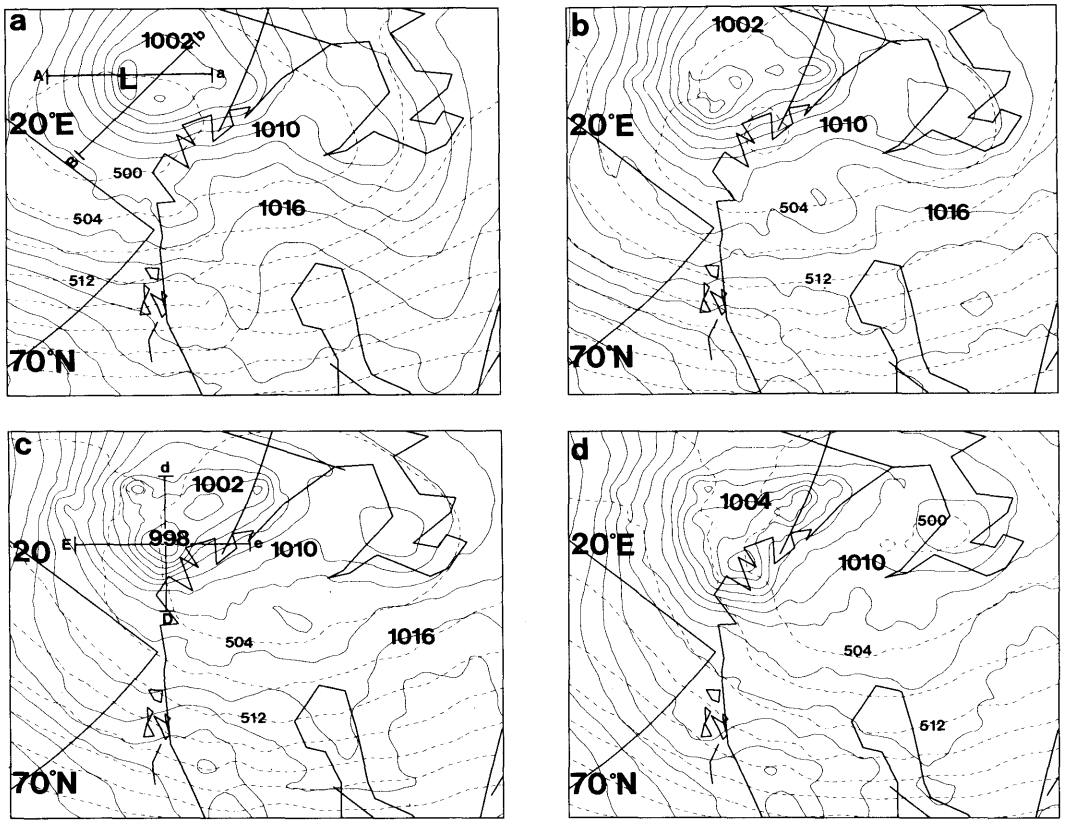

Fig. 9. Mean sea level pressure at contour intervals of 2 hPa (full lines) and geopotential height of 500 hPa (dash-dot lines) at contour intervals of 40 m after 6 h (a), 12 h (b), 15 h (c) and 18 h (d) of integration. Location of sections for Fig. 11 (Aa and Bb) is found in (a), while location of sections for Fig. 15 (Dd and Ee) is found in (c).

The fluxes are largest on the western flank of the parent low where the winds are strong. This distribution of surface fluxes, as well as the cold air advection, contributes to a direct secondary flow approximately perpendicular to the isobars. This can be seen mathematically from the Eliassen-Sawyer equation with the inclusion of diabatic heating (e.g., in Keyser and Shapiro, 1986), or understood qualitatively since a cross frontal circulation with warm air raising (adiabatic cooling) and cold air sinking (adiabatic warming) must be set up to retain thermal wind balance and couteract the frontogenesis. The cross-sections perpendicular to the frontal zone shown in Fig. 11 actually demonstrate that this is the case. There is a direct circulation all along the front, but it is deeper (extends up to 500 hPa) and stronger in the vicinity of the newly formed mesoscale low

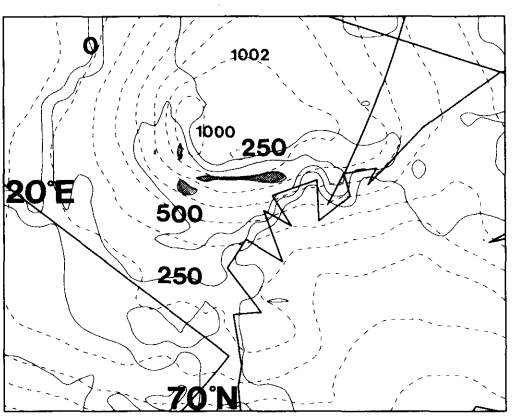

Fig. 10. Mean sea level pressure at contour intervals of 2 hPa (dash-dot lines) and surface fluxes of sensible and latent heat (added) at contour intervals of 250 W/m^2 (full lines). Areas with fluxes over 750 W/m^2 are shaded.

(Fig. 11a) than along the southern cross-section (Fig. 11b). Even further away from the forming mesoscale low the circulation is even more shallow (not shown). To understand the dynamics of the low, it is important to understand whether the frontal circulation is internal, caused by the deepening low, or an external feature is causing the low to deepen. The baroclinicity is strong (and shallow) all along the frontal zone and the low level stability is low with a layer of more "normal" stratification aloft. Wiin-Nielsen (1989) has studied such a configuration with a three-level quasi-nondivergent model and found that the low stability of the lowest layer (close to an adiabatic lapse rate) gives a maximum instability for wave lengths of 100 to 200 km, while slightly smaller lapse rates (more stable) give a maximum growth rate for wavelengths close to 500 km. The main activity is confined to low levels. In this case, however, the circulation is so deep that one is tempted to look for another explanation.

Fig. 12 shows the isentropic potential vorticity (IPV) at the 278 K isentropic surface at 1200 UTC 26 February 1987. The 278 K surface in the region is situated in a stable layer close to or above the tropopause between 500 and 550 hPa. There is a large scale IPV anomaly situated to the west of the synoptic scale cyclone, but we also notice that a small scale anomaly is superimposed on this large scale anomaly where the polar low starts to develop. An IPV anomaly will set up a horizontal as well as a vertical circulation. Ascending vertical motion is found where there is positive potential vorticity advection. From Fig. 12 we notice that the small scale anomaly may be responsible for the deep circulation seen in Fig. 11a. The large scale anomaly on the other hand is not contributing to the vertical motion in the area of interest. In our case the conditions are quite complicated consisting in a combination of an upper-level IPV anomaly with a complex low level anomaly made up by a pronounced low level circulation *and* a low-level warm anomaly. As discussed by Hoskins et al. (1985) a warm surface potential temperature anomaly is equivalent to a cyclonic IPV anomaly concentrated at the surface. In our case the two types of anomalies reinforce each other and give rise to a significant combined low-level IPV anomaly. Provided the upper-level anomaly comes close enough to the low level anomaly the two may interact forming a deep circulation like that seen in Fig. 11a.

In order for the vertical circulation set up by an upper-level potential vorticity anomaly to penetrate to low levels of the troposphere, the stability has to be small. Since small stability is connected to small values of the potential vorticity one obtains the conceptual model that an IPV

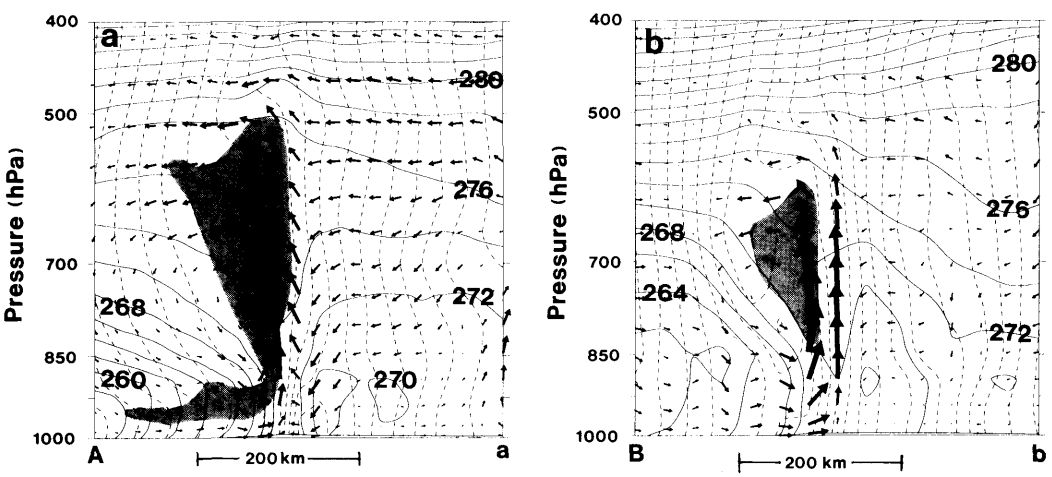

Fig. 11. Cross sections showing equivalent potential temperatures (full lines) at contour intervals of 2 K, absolute momentum (stippled lines) at contour intervals of 5 ms^{-1} and tangential air flow (arrows) after 6 hours of integration valid at 1800 UTC 26 February 1987. The length of an arrow corresponds to a 30 min trajectory. The shaded regions have relative humidity above 90%. (a) Section Aa. (b) Section Bb. Positions of sections are found in Fig. 9a.

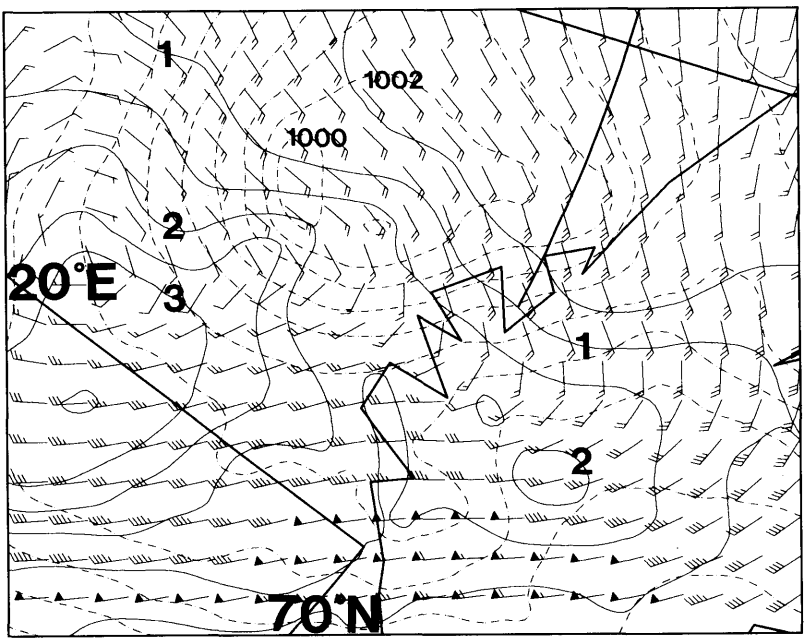

Fig. 12. Full lines are potential vorticity at the 278 K isentropic surface from 1200 UTC 26 February 1987, at contour intervals of 0.5 potential vorticity units (PVU) (1 PVU = 10^{-6} m^2 s^{-1} K kg^{-1}). Also shown are horizontal winds at the 278 K surface valid at the same time, a flag is 25 ms^{-1}, a full barb is 5 ms^{-1} and a half barb is 2.5 ms^{-1}. Dash-dot lines are mean sea level pressure at contour intervals of 2 hPa valid at 1800 UTC 26 February (i.e., 6 h later).

anomaly is required to give vertical circulation, but it becomes strong only if the induced vertical ascend is established in a region of low potential vorticity. Observations (Emanuel, 1988) and numerical simulations show that the vertical circulation tends to be aligned along absolute momentum surfaces. For the present case, the vertical circulation in strongest where the potential vorticity is small, and tends to follow the absolute momentum surfaces. The absolute momentum (M) is defined as $M = fx + v_n$, where v_n is the wind-component perpendicular to a cross-section and x is the distance along the cross-section. M is conserved for two-dimensional nonviscous flow. In Fig. 11a, the absolute momentum contours are shown together with equivalent potential temperature, and we notice that the (moist) potential vorticity is small in the region of strongest vertical velocities. A qualitative measure of (moist) potential vorticity can be found by counting the number of intersection points between the contours of absolute momentum and (equivalent) potential temperature in an unit area in the cross-section. The moist potential vorticity measures the stability when the air is saturated.

Potential vorticity is conserved for adiabatic nonviscous motion. Release of latent heat is a sink of potential vorticity above the diabatic heating maximum and a source below, contributing to a low stability and hence strong circulation above the heating. In an experiment with the release of latent heat was turned off (not shown) a much weaker circulation and development was obtained as compared to the experiment including latent heat release. In particular, the vertical circulation is not as deep as in Fig. 11a and the potential vorticity in the outflow region is not as small. In order to have intensification through surface pressure fall the upper level divergence must be larger than the lower level convergence (Van Delden, 1989ab). This is obtained if the diabatic heating through latent release makes the upper level IPV approach zero. In that case the M- and θ-surfaces will come close together which will facilitate the outflow

because air parcels, moving along the absolute momentum surfaces, will hardly have to deviate from the prevailing θ-surfaces.

In a recent paper, Montgomery and Farrel (1991) studied various initial conditions for cyclone developments in a semigeostrophic model with latent heat release. In addition to the "classical" strong baroclinic development where an upper level anomaly couples with a low level anomaly so that they mutually intensify, they found another class of disturbances which grows from potential vorticity generation at low levels due to latent heat released in ascent regions. These developments are slow in comparison to the classical type, but are not dependent on the presence of large amplitude perturbations. They suggest that (some) polar low developments consist of an initial baroclinic growth phase followed by a prolonged slow intensification due to diabatic effects. Van Delden (1989a) demonstrated that an axisymmetric cyclone in an Arctic environment may grow from diabatic processes (sensible heat from the ocean and release of latent heat) and a subsequent gradient wind adjustment providing a finite amplitude disturbance is present. The surface pressure drop is of the order of 0.2 hPa/h for a barotropic vortex. The deepening rate roughly doubles for a baroclinic vortex (the wind decreases with height). These numbers are roughly the same as those found for this polar low. For the present case the upper level forcing is hardly detectable after the first 6 hours of integration. Between 3 and 6 h into the integration, the central pressure drops by 2 hPa, while it drops by another 2 hPa during the next 9 h. These numbers combined with the lack of an upper level forcing after the initial stage, indicates that the theories of Montgomery and Farrel (1991) and Van Delden (1989a) may be applicable to this polar low development.

4.2. *Release of latent heat*

In Subsection 4.1, we discussed the importance of release of latent heat in creating low potential vorticity in the outflow region of the low. Diabatic heating through release of latent heat can take place through stable "forced" ascending motion, but also through convection. In the actual case there is strong precipitation all along the "frontal zone" of the parent low where the polar low develops. The maximum precipitation rate is found in the areas of the strongest vertical velocities, but precipitation is also found elsewhere, showing that parameterized convection contributes to the overall precipitation pattern for this case. To understand the spin-up of the low through destruction of IPV in the outflow regions as described in the previous section, the spatial distribution of latent heating must be explained. If latent heating (including the contribution from the convection) was to take place over a large region, the heating would be out of phase with the growing vortex inhibiting the development. Fig. 13 shows horizontal surface air (i.e., lowest model level) trajectories starting at 12 UTC 26 February 1987 ending at 03 UTC 27 February 1987 in the region of heavy precipitation. The numbers shown along the trajectory are equivalent potential temperatures of the air parcel every 3 hrs. One notices that air parcels following these trajectories experience considerable "heating rates" from surface fluxes of latent and sensible heat. Similar heating rates were found in Nordeng (1990) for one of the lows studied in that case. In order for deep convection to develop in the central region of the polar lows air parcels must acquire large amounts of heat and moisture from the surface as they spin towards the centre. Fig. 14 shows vertical soundings along the trajectory. The air is extremely stable when it leaves the ice, but rather

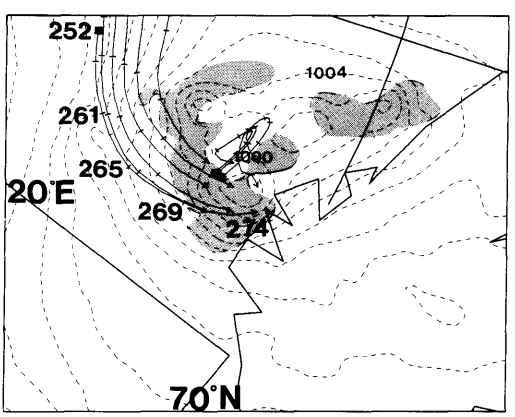

Fig. 13. Surface air trajectories ending up in the vicinity of the low at 0300 UTC 27 February 1987. The numbers along the trajectory are equivalent potential temperature after 0, 6, 9, 12 and 15 h of integration. Areas with heavy precipitation (> 1 mm/3 h) are stippled. Mean sea level pressure after 15 hours of integration valid at 0300 UTC 27 February 1987 is indicated by stippled lines at contour intervals of 2 hPa.

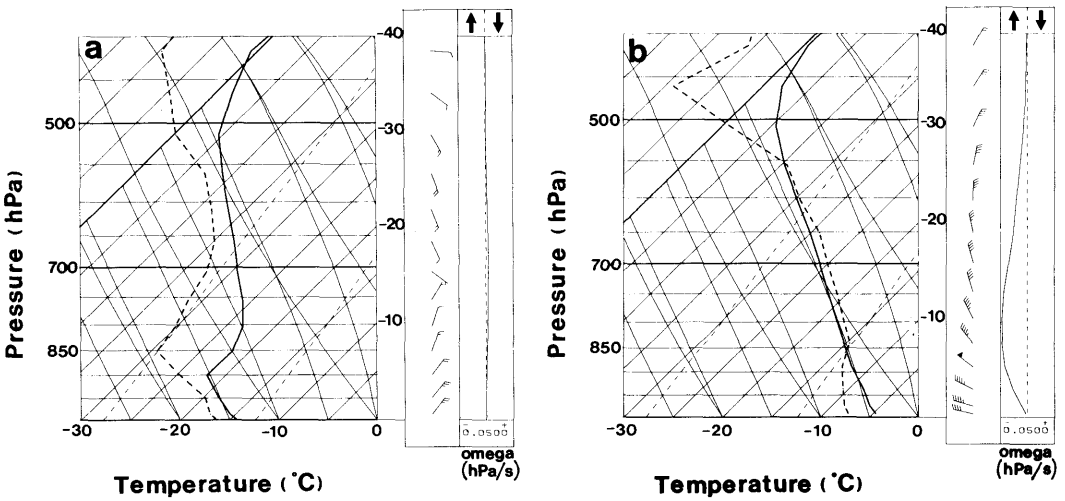

Fig. 14. Soundings taken from the model simulation after (a) 6 h and (b) 15 h of integration along the trajectory in Fig. 15. Temperature and dew point temperature are plotted in skew tephigrams with lines of constant temperature running upwards to the right. The arrows are wind direction (north is up) and speed (a flag is 25 ms^{-1}, a full barb is 5 ms^{-1} and a half barb is 2.5 ms^{-1}). The vertical velocity, omega (hPa s^{-1}) is visualized besides the winds.

quickly destabilizes due to sensible heat fluxes from the "warm" ocean (Fig. 14a). When the air enters the updraught regions (Fig. 14b) it is marginally stable. The low stability favours strong vertical motion. We notice that there is a capping inversion on the soundings of Fig. 14a. We think that this inversion is important in localizing the spatial distribution of the heating. First of all, the capping inversion limits the amount of air to be heated so that the temperature can increase considerably. Furthermore, convection is not taking place over the whole region, but is localized

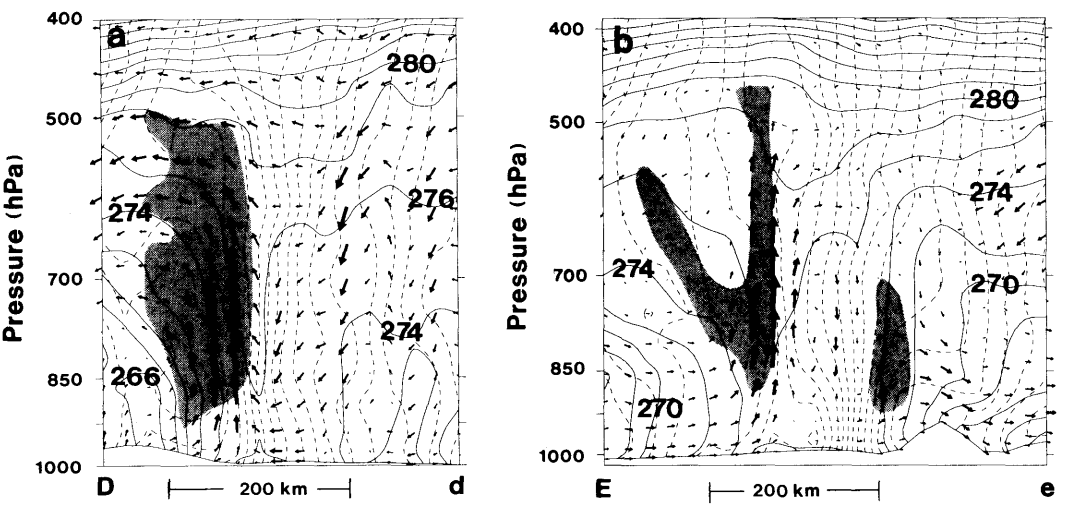

Fig. 15. Cross sections showing equivalent potential temperatures (full lines) at contour intervals of 2 K, absolute momentum (stippled lines) at contour intervals of 5 ms^{-1} and tangential air flow (arrows) after 15 hours of integration valid at 0300 UTC 27 February 1987. The length of an arrow corresponds to a 15-min trajectory. The shaded regions have relative humidity above 90%. (a) Section Dd. (b) Section Ee. Positions of sections are found in Fig. 9c.

to the areas in the vicinity of the mesoscale low. Økland (1989) advocates that such a phenomenon is the main factor determining the scale and location of the polar low developments. It may sound surprisingly that air from the "cold side" of the cyclone feeds the updraughts. However, a similar structure was found when simulating a major large scale extratropical low off the North American east coast (Melvin Shapiro, personal communication).

It should also be emphasized that the low level air near the vicinity of the polar low centre, where the advection is small, increases its equivalent potential temperature during the integration so that there is a gradual destabilizing of the air even without transport of moistened and heated air from the surroundings. The increase of equivalent potential temperature is either a result of surface fluxes in the cyclone centre or from adiabatic warming due to subsidence. Even though the winds are small here, the surface exchange coefficients (Louis et al., 1981) are written so that in the limit of no winds there are still surface fluxes from free convection. Van Delden (1989a) argues that the contribution from sensible heat flux in polar lows plays the same role as release of latent heat, because it affects the hydrostatic pressure distribution.

Fig. 15 shows cross-sections through the centre of the low at 03 UTC 27 February. We notice that the air is neutrally stable to slantwise convection in the region of strong vertical velocity and that the air parcels closely follow the absolute momentum surfaces. The air is convectively unstable in those regions of the low where the vertical velocity of the model is weak. This gives an effective heating from release of latent heat in a ring around the whole cyclone centre from grid resolved condensation where the vertical velocity is strong or from convection elsewhere. Fig. 16 shows the temperature and relative humidity in the cross sections. There is a clear "eye" in the centre of the cyclone with a heavy "cloud-band" around the centre. From these sections it is possible to verify the model simulation by comparing cloud top and surface temperatures as retrieved from satellites. In fact, it is verified that the model simulates closely the observed temperatures retrieved from the NOAA-9 on orbit #11379, 27 February 1987 at 0411 UTC (recorded on HRPT data received at Dundee University, Dundee Scotland, published by

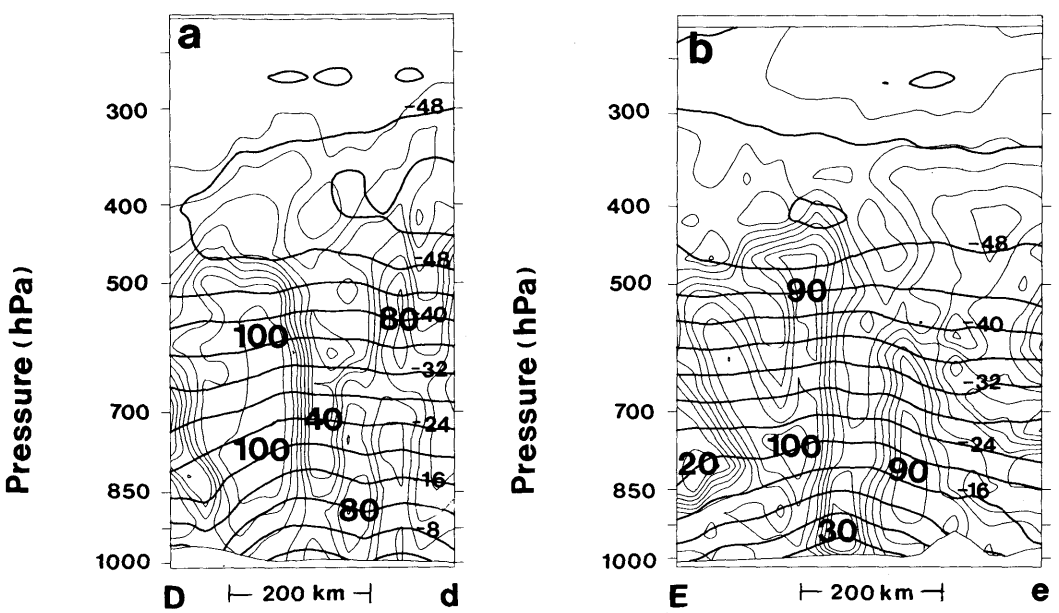

Fig. 16. Cross sections showing absolute temperatures (full lines) at contour intervals of 2 K and relative humidity at contour intervals of 10% after 15 h of integration valid at 0300 UTC 27 February 1987. (a) Section Dd, (b) Section Ee. Positions of sections are found in Fig. 9c.

Twitchell et al., 1989) with a −18°C stratocumulus cloud deck in the cold air outbreak west of the low, cloud top temperatures varying from −43°C to −38°C in the heavy cloud deck around the eye and −3°C to +2°C in the eye.

5. Discussion and summary

A particularly beautiful polar low has been studied in order to understand the mechanisms for its development. Polar lows have been classified as the high latitude version of tropical cyclones, and indeed, the satellite images of this low shows a strikingly similarity to a tropical cyclone. It is remarkably symmetric, has a clear spiral band structure and a well defined eye. One of the objectives of this study was to investigate whether the low really could be classified as an "arctic hurricane". To do this we employed conventional observations as well as satellite images, but also direct model output from a mesoscale numerical weather prediction model. The later proved very successful, in that the development of the low could be studied in detail from the high spatial and temporal data set from the model.

We did find several similarities between this low and tropical cyclones. The model simulation shows that the air flow within the low has several simularities with that observed in tropical cyclones. The low intensifies over the sea and quickly decays when entering land. There is a strong cyclonic (Fig. 17a) inflow at low levels, ascending motion in a band around a central part with subsidence (the eye), and anticyclonic outflow close to the tropopause (Fig. 17b). The core is warm and there is a vertical distribution of equivalent potential temperature within the core which is similar to that found in tropical cyclones. The relative humidity of the eye is lower than that of the surroundings, giving a cloud free eye. According to Anthes (1982 p. 29): "*The eye is a part of cyclone structure that is crucial to the generation of extremely low pressures and intense wind speeds in hurricanes*". *The subsidence in the eye region plays a particularly important role. It implies adiabatic warming and subsequently low central pressure*". However, even in this case where we observe a well defined eye we do not find exceptionally low surface pressures. Rasmussen (1989) discusses the effect of adiabatic warming of the air from subsidence in the eye. Because of the low moisture content of the cold arctic air relative small differences between moist adiabatic ascend (cooling) and dry adiabatic descend (warming) can be expected. Van Delden (1989b) discusses the role of the eye size for the intensification of cyclones driven by diabatic processes and shows that deepening of a cyclone is strongly inhibited if the heating is located dynamically too far away from the cyclone centre. The relevant parameters are the size of the eye and the Rossby radius of deformation defined in Van Deldens model as

$$\mathrm{Ro} = \sqrt{\frac{\Delta\rho}{\rho}\frac{gh}{2}}\frac{1}{\eta + f},$$

where $\Delta\rho$ is the difference in density between the upper and lower part of the cyclone, h is approximately half the depth of the cyclone and η is the relative vorticity. For the present cyclone after 15 h of integration, Ro is estimated to be close to 75 km while the eye radius is approximately 75 km as well. This is an optimum configuration for intensification. The apparent "large" eye is in fact the "right" size for further development.

The air just outside the eye is more or less saturated and the stratification is moist adiabatic along surfaces of constant absolute momentum. Similar structures were found to develop in simulations of tropical hurricanes and polar lows with axisymmetric models (Rotunno and Emanuel, 1987; Emanuel and Rotunno, 1989). Even further out from the centre, the model simulation and satellite images as well show shallow convection confined to low levels by a capping inversion. We have stressed that this inversion may be important for the development of the low, because it hinders deep convection to develop everywhere. The convection has to be organized to have a significant effect on the large scale flow. The capping inversion allows a shallow layer of air close to the surface to be heated and moistened to the point of instability release. Had the air been heated over a deep layer it might never reached this point.

The precursor of the polar low was a synoptic scale cyclone which re-intensified in its rear part due to an approaching upper level potential vorticity (IPV) maximum associated with a perturbation on the major upper level trough belonging to the parent low. The induced upper level circulation coupled with the low level circulation and the low level temperature anomaly, both created from the

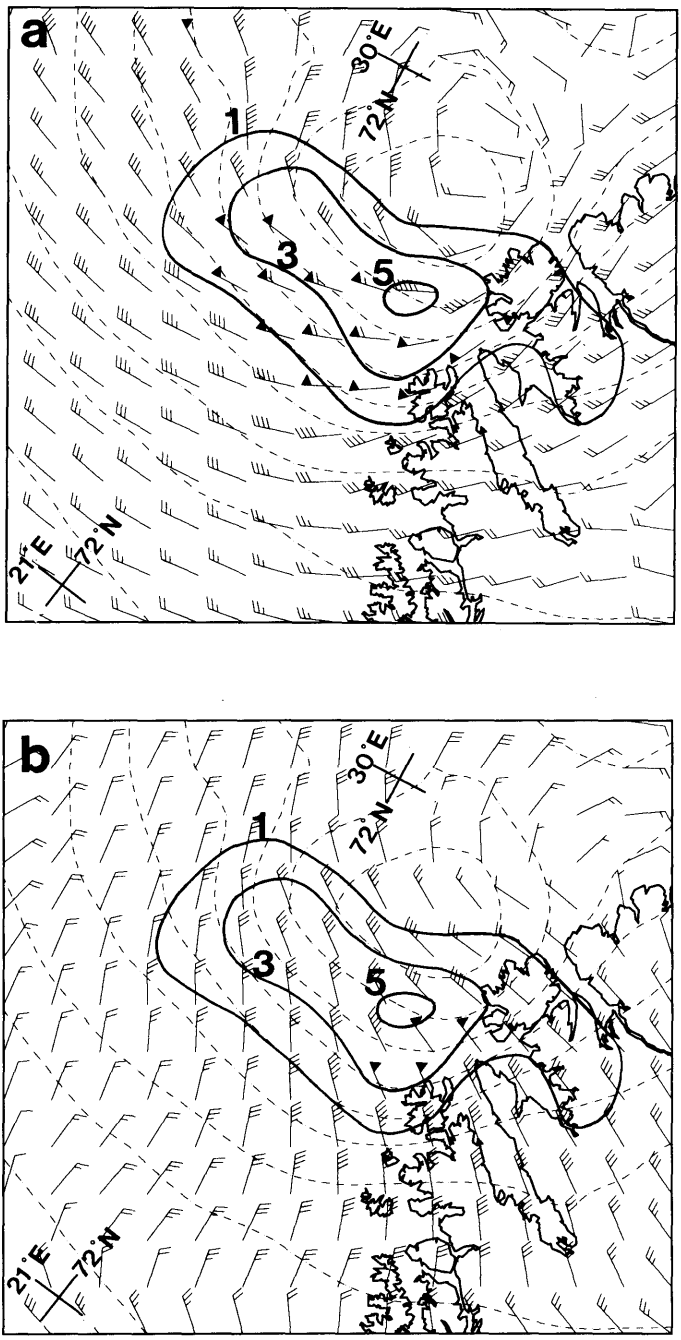

Fig. 17. Winds at 925 hPa (a) and at 500 hPa (b). A flag on the wind arrows denotes a wind speed of 25 ms^{-1}, a full barb is 5 ms^{-1} and a half barb is 2.5 ms^{-1}. Full lines are contours of vertical velocity (dPa s^{-1}) at 700 hPa in the region of largest ascending motion. Contours of mean sea level pressure (dashed lines) at contour intervals of 2 hPa are shown to demonstrate the position of the centre of the low. The inner isobar is 998 hPa.

parent low. A deep circulation developed resulting in latent heat release in the ascending regions. This in turn destroyed potential vorticity aloft leading to an increased upper level outflow and eventually to surface pressure fall. Such a feature is hardly seen in the tropics, but it is known that cyclones which are driven by latent heat release are finite amplitude instabilities such that a disturbance of some finite amplitude has to be present for the cyclone to start growing (Emanuel, 1989; Van Delden, 1989ab). There are indications that unusual strong intensifications of some tropical cyclones can be explained from interactions with extratropical upper level cold troughs. Simpson and Riehl (1981) describe how tropical cyclone Camille twice benefitted from upper cold core troughs, first as it underwent the transition from a tropical disturbance to a tropical cyclone and next as it transformed from a moderate to an extremely strong cyclone.

The polar low discussed in this paper bear some resemblance to other strong cyclones which form over water. Rasmussen and Zick (1987) for example documented a warm core cyclone in the Mediterranean Sea which had several similarities with the low studied here particularly with respect to the cloud structure. Shapiro et al. (1990) show from aircraft observations and model simulations that the most intense part of some extratropical cyclones is found along the so called bent-back warm front which curves towards the centre of the low from the intersection point between the warm and cold fronts. Along this front they observe a secondary development. According to Shapiro et al. (1990): "*In addition, these simulations and observations describe the formation of shallow, warm-core, mesoscale cyclonic circulation of the parent cyclones. These internal circulations bear a striking resemblance to the polar-low, mesoscale, extratropical cyclones observed and simulated within polar air streams over the Arctic and Atlantic Oceans*". In fact, the polar low development described here in some ways looks very similar to the low studied by Shapiro et al. (1990) except that the scale of the polar low is smaller. In both cases there is frontogenesis from cold air advection west of the large scale occluded low and an intensification along this newly formed front.

The development discussed in this paper was triggered by an upper level potential vorticity anomaly in a region of strong low level baroclinicity. To our knowledge, a polar low development without an initial upper level forcing has not been documented in the literature. In addition, simulations of polar lows show that most of them are crucially dependent on release of latent heat during later stages of their development. A main driving mechanism is therefore surely release of latent heat while the triggering mechanism is release of baroclinic energy.

In this study we have documented several similarities between tropical cyclones in general and a particular polar low. Whether this is sufficient to classify this polar low as a high latitude version of a tropical cyclone remains a question of opinion. At least this polar low seems to belong to the class of cyclones which are partly driven by the release of latent heat. Theories for such cyclones are found, e.g., in Emanuel (1986), Van Delden (1989ab) and Montgomery and Farrel (1991).

REFERENCES

Anthes, R. A. 1982. Tropical Cyclones. Their Evolution, Structure and Effects. *Meteorological Monograms 19*, American Meteorological Society.

Blackadar, A. K. 1979. *High resolution models of the planetary boundary layer. Advances in environment and scientific engineering.* London: Gordon and Breach. 276 pp.

Bratseth, A. M. 1982. A simple and efficient approach to the initialization of weather prediction models. *Tellus 34*, 352–357.

Bratseth, A. M. 1983. Some economical explicit finite difference schemes for the primitive equations. *Mon. Wea. Rev. 111*, 663–668.

Bratseth, A. M. 1986. Statistical interpolation by means of successive corrections. *Tellus 38A*, 449–457.

Emanuel, K. A. 1986. An air-sea interaction theory for tropical cyclones. Part I: Steady-state maintenance. *J. Atmos. Sci. 43*, 585–604.

Emanuel, K. A. 1988. Observational evidence of slantwise convective adjustment. *Mon. Wea. Rev. 116*, 1805–1816.

Emanuel, K. A. 1989. The finite-amplitude nature of tropical cyclogenesis. *J. Atmos. Sci. 46*, 3431–3456.

Emanuel, K. A. and Rotunno, R. 1989. Polar lows as arctic hurricanes. *Tellus 41A*, 1–17.

Geleyn, J.-F. 1985. On a simple parameter-free partition

between moistening and precipitation in the Kuo scheme. *Mon. Wea. Rev. 113*, 406–407.

Grønås, S. and Hellevik, O. E. 1982. *A limited area prediction model at the Norwegian Meteorological Institute.* Techn. Rep. no. 61, Norwegian Meteorological Institute, Oslo, Norway.

Grønås, S. and Midtbø, K. H. 1987. Operational multivariate analyses by successive corrections. Proceedings: Collection of papers presented at the *WMO/IUGG NWP Symposium*, Tokyo, 4–8 August 1986. Meteorol. Soc. Japan.

Hoskins, B., McIntyre, M. E. and Robertson, A. W. 1985. On the use and significance of isentropic potential vorticity maps. *Quart. J. Roy. Meteorol. Soc. 111*, 877–946.

Keyser, D. and Shapiro, M. A. 1986. A review of the structure and dynamics of upper-level frontal zones. *Mon. Wea. Rev. 114*, 452–499.

Keyser, D. and Uccellini, L. W. 1987. Regional models: Emerging research tools for synoptic meteorologists. *Bull. Amer. Meteor. Soc. 68*, 306–320.

Louis, J.-F., Tiedtke, M. and Geleyn, J.-F. 1981. A short history of the PBL-parameterization at ECMWF. Proceedings from: *Workshop on planetary boundary layer parameterization.* European Centre for Medium range Weather Forecasts. Shinfield Park, Reading, England.

Montgomery, M. T. and Farrel, B. F. 1991. Moist surface frontogenesis associated with interior potential vorticity anomalies in a semigeostrophic model. *J. Atmos. Sci. 48*, 343–367.

Nordeng, T. E. 1986. *Parameterization of physical processes in a three-dimensional numerical weather prediction model.* Techn. Rep. no. 65. Norwegian Meteorological Institute, Oslo, Norway.

Nordeng, T. E. 1990. A model-based diagnostic study of the development and maintenance mechanism of two polar lows. *Tellus 42A*, 92–108.

Nordeng, T. E., Reistad, M. and Magnusson, A. K. 1988. *An optimum use of atmospheric data in wind wave modelling, numerical experiments.* Techn. Rep. no. 68. Norwegian Meteorological Institute, Norway.

Økland, H. 1977. On the intensification of small-scale cyclones formed in very cold air masses heated by the ocean. Institute Report Series, No. 26. Institute for Geophysics, University of Oslo, Norway.

Økland, H. 1989. On the genesis of polar lows. In: *Polar and Arctic lows*, eds. P. F. Twitchell, E. Rasmussen and K. L. Davidson. A Deepak Publishing, Vi., USA, 179–190.

Rasmussen, E. 1977. *The polar low as a CISK-phenomenon.* Report no. 6. University of Copenhagen, Denmark, Institute for Theoretical Meteorology, 78 pp.

Rasmussen, E. 1979. The polar low as an extratropical CISK disturbance. *Q. J. R. Meteorol. Soc. 105*, 531–545.

Rasmussen, E. 1989. A comparison study of tropical cyclones and polar lows. In: *Polar and arctic lows*, eds. P. F. Twitchell, E. Rasmussen and K. L. Davidson. A Deepak Publishing, Vi., USA, 47–80.

Rasmussen, E. and Zick, C. 1987. A subsynoptic vortex over the Mediterranean with some resemblance to polar lows. *Tellus 39A*, 408–425.

Rotunno, R. and Emanuel, K. A. 1987. An air-sea interaction theory for tropical cyclones. Part II: Evolutionary study using a nonhydrostatic axisymmetric model. *J. Atmos. Sci. 44*, 542–561.

Shapiro, M. A., Donall, E. G., Neiman, P. and Fedor, L. 1990. On the mesoscale structure of extratropical marine cyclones. Extended abstracts from *The 4th Conference on Mesoscale Processes*, Boulder, Co. 25–29 June 1990. Amer. Meteorol. Soc., Boston. Ma., USA.

Simpson, R. H. and Riehl, H. 1981. *The hurricane and Its impacts.* Louisiana State University Press. Baton Rouge and London. 398 pp.

Twitchell, P. F., Rasmussen, E. and Davidson, K. L., (eds.). 1989. *Polar and arctic lows.* A Deepak Publishing, Vi., USA, 420 pp.

Van Delden, A. 1989a. Gradient wind adjustment, CISK and the growth of polar lows by diabatic heating. In: *Polar and arctic lows*, eds. P. F. Twitchell, E. Rasmussen and K. L. Davidson. A Deepak Publishing, Vi., USA, 109–130.

Van Delden, A. 1989b. On the deepening and filling of balanced cyclones by diabatic heating. *Meteorol. Atmos. Phys. 41*, 127–145.

Wiin-Nielsen, A. 1989. On the precursor of polar lows. In: *Polar and arctic lows*, eds. P. F. Twitchell, E. Rasmussen and K. L. Davidson. A Deepak Publishing, Vi., USA, 420 pp.